Acta Crystallographica Section D
Biological Crystallography
ISSN 0907-4449

Anatomy of secretin binding to the *Dickeya dadantii* type II secretion system pilotin

Saima Rehman,[a] Shuang Gu,[a] Vladimir E. Shevchik[b]* and Richard W. Pickersgill[a]*

[a]School of Biological and Chemical Sciences, Queen Mary University of London, Mile End Road, London E1 4NS, England, and [b]Université de Lyon, 69003 Lyon; Université Lyon 1, 69622 Lyon; INSA-Lyon, 69621 Villeurbanne; CNRS, UMR5240, Microbiologie Adaptation et Pathogénie, 69622 Lyon, France

Correspondence e-mail: vladimir.shevchik@insa-lyon.fr, r.w.pickersgill@qmul.ac.uk

Received 25 January 2013
Accepted 19 March 2013

PDB Reference: secretin–pilotin complex, 3uym

The secretins are a family of large multimeric channels in the outer membrane of Gram-negative bacteria that are involved in protein export. In *Dickeya dadantii* and many other pathogenic bacteria, the lipoprotein pilotin targets the secretin subunits to the outer membrane, allowing a functional type II secretion system to be assembled. Here, the crystal structure of the C-terminal peptide of the secretin subunit bound to its cognate pilotin is reported. In solution, this C-terminal region of the secretin is nonstructured. The secretin peptide folds on binding to the pilotin to form just under four turns of α-helix which bind tightly up against the first helix of the pilotin so that the hydrophobic residues of the secretin helix can bind to the hydrophobic surface of the pilotin. The secretin helix binds parallel to the first part of the fourth helix of the pilotin. An N-capping aspartate encourages helix formation and binding by interacting favourably with the helix dipole of the helical secretin peptide. The structure of the secretin–pilotin complex of the phytopathogenic *D. dadantii* described here is a paradigm for this interaction in the OutS–PulS family of pilotins, which is essential for the correct assembly of the type II secretion system of several potent human adversaries, including enterohaemorrhagic *Escherichia coli* and *Klebsiella oxytoca*.

1. Introduction

Secretins are integral membrane proteins which assemble to form multimeric secretion channels in the outer membrane for the passage of secreted proteins or protein complexes. They are found in the type II secretion system (T2SS), the type III secretion system, the type IV pilus system and the filamentous phage-extrusion machinery (Thanassi & Hultgren, 2000; Peabody *et al.*, 2003; Filloux, 2004; Korotkov, Gonen *et al.*, 2011). The T2SS secretes folded proteins and protein complexes into the environment. The outer membrane secretin of the T2SS has been shown to form a dodecameric pore using transmission electron microscopy and single-particle image reconstruction (Chami *et al.*, 2005; Reichow *et al.*, 2010). The first of these two papers may also provide a low-resolution glimpse of the secretin–pilotin complex, which is possibly observed as radial spikes protruding from the pore (Chami *et al.*, 2005). In the T2SS the outer membrane complex docks onto the inner membrane platform. The associated cytoplasmic ATPase energizes secretion by causing the assembly of a pilus within the periplasmic space, resulting in the secretion of selected proteins into the external milieu

© 2013 International Union of Crystallography
Printed in Singapore – all rights reserved

(Douzi *et al.*, 2012; Korotkov *et al.*, 2012). The outer membrane complex comprises the secretin plus its lipoprotein pilotin, which is anchored in the outer membrane by a covalently attached lipid. The T2SS secretin comprises four N-terminal domains (N0 and N1–N3), the secretin domain and the C-terminal S-domain (Fig. 1; Bayan *et al.*, 2006; Reichow *et al.*, 2010). The S-domain is essential for the secretin to engage with the targeting pathway that delivers the secretin to the outer membrane (Hardie *et al.*, 1996; Sandkvist, 2001). In the absence of the pilotin the oligomeric complex does not assemble in the outer membrane but instead assembles in the inner membrane (Shevchik & Condemine, 1998; Guilvout *et al.*, 2006). The S-domain of the secretin subunit binds to the lipoprotein pilotin, which in turn engages the Lol machinery, resulting in the trafficking of the secretin from the inner membrane to the outer membrane (Tokuda & Matsuyama, 2004; Collin *et al.*, 2011; Okuda & Tokuda, 2011). The N0 domain then docks the secretin to the inner membrane platform (Login *et al.*, 2010; Korotkov, Johnson *et al.*, 2011; Berry *et al.*, 2012; Gu, Kelly *et al.*, 2012; Wang *et al.*, 2012).

Recent phylogenetic analysis (Strozen *et al.*, 2012; Dunstan *et al.*, 2013) has demonstrated three groups of secretins, one of which, the so-called *Klebsiella* type, includes OutD from *Dickeya dadantii*, PulD from *Klebsiella* and GspD from enterohaemorrhagic *Escherichia coli*. The corresponding pilotins, PulS, OutS and GspS, respectively, share significant sequence homology and their structures are therefore closely similar (PDB entries 3utk, 4a56 and 3sol, respectively; S. Gu, S. Rehman, X. Wang, V. E. Shevchik & R. W. Pickersgill, unpublished work; Tosi *et al.*, 2011; K. V. Korotkov & W. G. J. Hol, unpublished work). A second family of pilotins, the *Vibrio* family, were identified which bind a cognate lipoprotein pilotin named AspS in *Vibrio* or YghG in enterotoxigenic *E. coli*. Despite its functional equivalence, the AspS pilotin (PDB entry code 4ftf; Dunstan *et al.*, 2013) is structurally distinct from the OutS–PulS family of pilotins.

Pilotins of the OutS–PulS family directly bind a short region within the S-domain of their cognate secretin (Nickerson *et al.*, 2011; Tosi *et al.*, 2011; Gu, Rehman *et al.*, 2012). In our previous study, we established using NMR spectroscopy that 18 residues at the C-terminal end (residues 691–708) of the secretin OutD were sufficient to bind the OutS pilotin with high affinity (Gu, Rehman *et al.*, 2012). NMR and CD analyses established that this C-terminal part of the secretin (the S-domain) was unstructured before binding but became helical on binding to the pilotin (Gu, Rehman *et al.*, 2012). A crystal of the pilotin with the 18-residue peptide bound contained both ordered and disordered protein, which hampered conventional refinement; nevertheless, we were able to use the crystallographic data and a nonconventional refinement methodology to provide an image of the binding of the secretin helix to the concave surface of the pilotin. The method used to effect refinement was to model partially ordered protein using a large number of water molecules. The structure of the pilotin–secretin complex presented was supported by results from NMR spectroscopy, fluorescence spectroscopy, circular-dichroism spectroscopy and mutagenesis.

Here, we have produced a new pilotin–secretin peptide complex crystal using a 15-residue peptide; the crystal is not obviously twinned and no substantial disorder is present. The crystal structure of this complex can therefore be refined using a conventional crystallographic refinement scheme and the molecular anatomy of the complex can be described in detail.

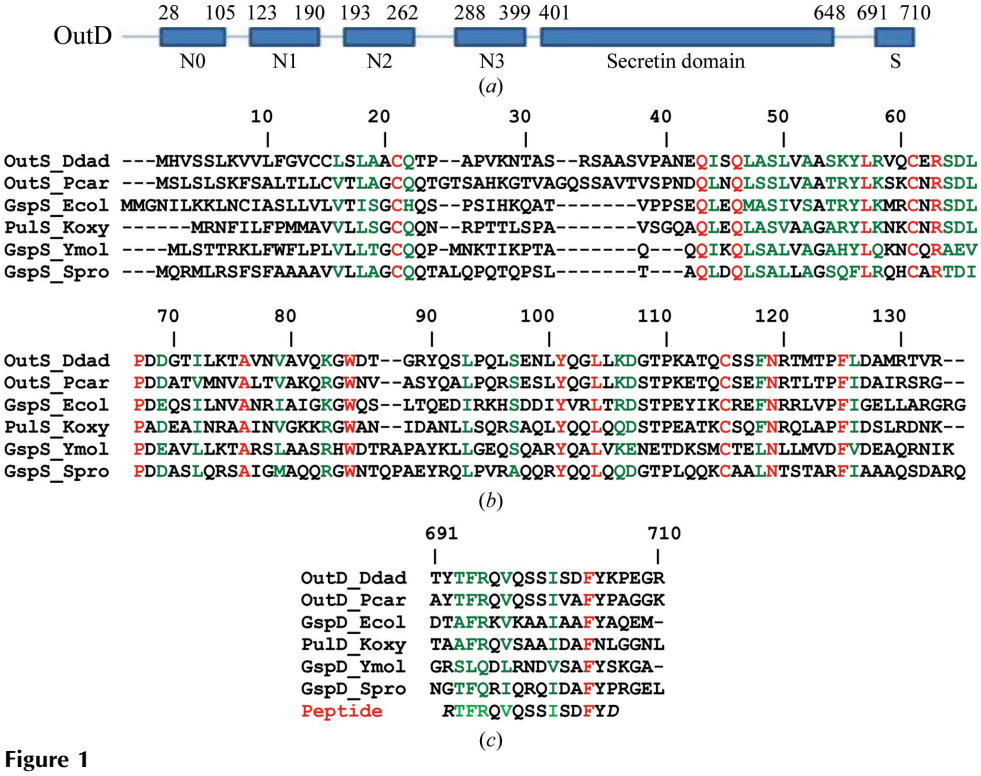

Figure 1
Alignments of the pilotin sequences and of the C-terminal region (S-domain) of their cognate secretins. (*a*) Overview of the domain structure of *D. dadantii* secretin (OutD) comprising N0, N1–N3, secretin and the S-domain. (*b*) Alignment of the *D. dadantii* OutS pilotin sequence with other members of the OutS–PulS family of pilotins. (*c*) Alignment of the *D. dadantii* OutD (S-domain) sequence with cognate secretins. Shown in the alignments are the pilotin and secretin homologues of *D. dadantii* (*Erwinia chrysanthemi* 3937; Q01567 and Q01565), *Pectobacterium carotovorum* (C6DAR0 and C6DAQ5), *Escherichia coli* O157:H7 (Q7BSV3 and Q9ZGU0), *Klebsiella oxytoca* (P20440 and P15644), *Yersinia mollaretii* (C4S9G3 and C4S9F5) and *Serratia odorifera* (D4E1I4 and A8GJQ5). Identical residues are shown in red and residues that are similar in character are shown in green. The sequence of the 15-residue peptide used in this crystallographic work is also shown.

2. Materials and methods

The pilotin was prepared as described previously (Gu, Rehman *et al.*, 2012). The secretin peptide *R*TFRQTFRQVQSSISDFY*D* was obtained from Zinsser Analytic (the residues added to aid solubility are shown in italics). A 1.1:1.0 molar ratio of peptide to pilotin was used in sitting-drop crystallization trials with a protein concentration of 18 mg ml^{-1}. Crystals of maximum dimension 0.2 mm were grown using 0.1 *M* Na HEPES buffer pH 7.5, 2% PEG 400, 2 *M* ammonium sulfate. Reservoir augmented with 25% glycerol was used as a cryoprotectant and X-ray diffraction data were collected to 2.1 Å resolution using a PILATUS 6M pixel detector on the PROXIMA1 beamline at the SOLEIL synchrotron, France. Data were processed using *XDS* (Kabsch, 2010) and *XDSME* and were scaled using *SCALA* (Evans, 2006). Data quality was assessed using $R_{\rm p.i.m.}$ (Weiss, 2001). The reduced data were analysed using *PHENIX* (Adams *et al.*, 2010), *REFMAC* (Murshudov *et al.*, 2011) and *Coot* (Emsley *et al.*, 2010), and the quality of the final model was assessed using *PROCHECK* (Laskowski *et al.*, 1993).

A MicroCal VP-ITC was used for thermodynamic assessment of binding. Pilotin and secretin peptide were dialysed against 30 m*M* Tris pH 8 in the same beaker to avoid heat-of-dilution effects. A reference power of 30 µcal s^{-1} was used (1 cal = 4.186 J) and the experiments were run at 303 K. 250 µl 175 µ*M* dialysed secretin peptide was titrated into 1.8 ml 25 µ*M* dialysed pilotin by 25 injections each of 10 µl (one injection every 300 s with constant stirring at 300 rev min^{-1}). For the control experiments, buffer was titrated into pilotin solution and secretin into buffer solution; these heat changes were negligible.

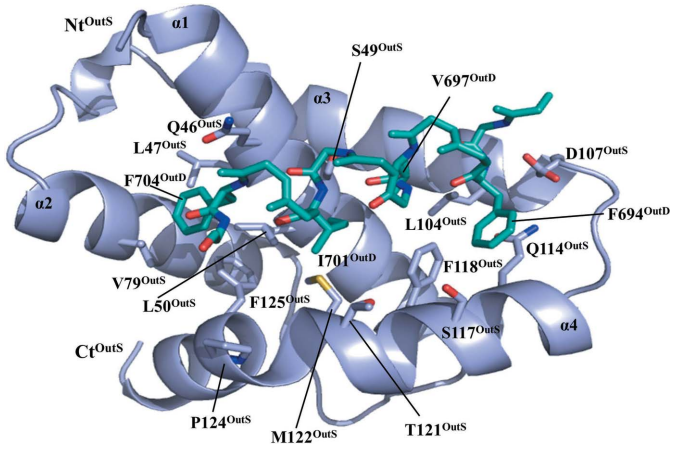

Figure 2
Structure of the *D. dadantii* pilotin–secretin peptide complex. The secretin helix is shown in cyan and binds to the pilotin (depicted in grey). Residues that are discussed in the text are drawn as sticks and labelled. The conserved hydrophobic residues of the secretin peptide bind to hydrophobic pockets either side of the first α-helix of the pilotin. The pilotin residues have the superscript OutS and the secretin residues have the superscript OutD. This figure and other figures depicting molecules were produced using *PyMOL* (DeLano & Lam, 2005).

Table 1
Data-collection and refinement statistics for the *D. dadantii* pilotin–secretin complex.

Values in parentheses are for the outer resolution shell. The values presented in this table are from *SCALA* (Evans, 2006), *REFMAC* (Murshudov *et al.*, 2011) and *PROCHECK* (Laskowski *et al.*, 1993) from the *CCP*4 suite.

Data collection	
Space group	$P6_522$
Unit-cell parameters (Å)	a = 53.60, c = 142.44
Molecules per asymmetric unit	1
Wavelength (Å)	0.98011
Resolution (Å)	47.48–2.15 (2.27–2.15)
Total No. of observations	57013 (8147)
No. of unique reflections	7209 (1009)
Multiplicity	7.9 (8.1)
Completeness (%)	100.0 (100.0)
$R_{\rm merge}$†	0.137 (0.804)
$R_{\rm p.i.m.}$‡	0.052 (0.300)
$\langle I/\sigma(I)\rangle$	9.1 (2.4)
Refinement	
Resolution limits (Å)	46.421–2.150
$R_{\rm work}/R_{\rm free}$§	0.2099/0.2760
R.m.s.d., bonds (Å)	0.015
R.m.s.d., angles (°)	1.6166
Wilson B factor (Å^2)	27.5
No. of protein atoms	861
No. of water molecules	14
Ramachandran plot statistics, residues in (%)	
Most favoured regions	98.1
Additional allowed regions	1.9

† $R_{\rm merge} = \sum_{hkl}\sum_i |I_i(hkl) - \langle I(hkl)\rangle|/\sum_{hkl}\sum_i I_i(hkl)$, where $I_i(hkl)$ is the intensity of the ith observation, $\langle I(hkl)\rangle$ is the mean intensity of the reflection and the summations extend over all unique reflections (hkl) and all equivalents (i), respectively. ‡ $R_{\rm p.i.m.}$ is a measure of the quality of the data after averaging the multiple measurements: $R_{\rm p.i.m.} = \sum_{hkl}\{1/[N(hkl)-1]\}^{1/2}\sum_i |I_i(hkl) - \langle I(hkl)\rangle|/\sum_{hkl}\sum_i I_i(hkl)$, where $N(hkl)$ is the multiplicity and the other variables are as defined for $R_{\rm merge}$ (Weiss, 2001). § R factor = $\sum_{hkl}||F_{\rm obs}| - |F_{\rm calc}||/\sum_{hkl}|F_{\rm obs}|$, where $F_{\rm obs}$ and $F_{\rm calc}$ represent the observed and calculated structure factors, respectively. $R_{\rm work}$ is calculated using the 95% of the data included in refinement and $R_{\rm free}$ is calculated using the excluded 5%.

3. Results and discussion

The *D. dadantii* pilotin (OutS) structure comprises four α-helices. The first two helices form an antiparallel hairpin, with the third and bent fourth helices at right angles to and wrapped around the first pair (Fig. 2). A single disulfide bridge is important in maintaining the structure. The OutS pilotin has a concave hydrophobic surface that is the binding site for the secretin S-domain. Conventional refinement of a previous complex, which was formed using an 18-residue peptide, was not possible because of the presence of disordered protein molecules. Refinement of this complex was only possible when the disordered protein was modelled using a large number of water molecules (Gu, Rehman *et al.*, 2012).

The crystals of the pilotin–secretin peptide complex reported in this paper belonged to space group $P6_522$ (Table 1) with one pilotin–secretin peptide complex in the asymmetric unit. The structure was solved by molecular replacement using the native structure of the pilotin protein (PDB entry 3utk; S. Gu, Rehman *et al.*, 2012). The structure of the complex refines to a model with reasonable stereochemistry and crystallographic residuals (Table 1). The coordinates of the pilotin–secretin peptide complex have been deposited in the PDB (PDB entry 3uym). Clear electron density defines residues 39^{OutS}–130^{OutS} of the pilotin structure; residues 38^{OutS} and

131^{OutS}–132^{OutS} are present but are not so clearly defined. Residues Thr2–Tyr14 of the 15-residue secretin peptide, corresponding to residues Thr693^{OutD}–Tyr705^{OutD} of the secretin OutD, are also clearly defined in the electron-density map (Fig. 3). The two additional residues added to the peptide to aid solubility, an arginine and an aspartate at the N- and C-termini, respectively, are present but are not clearly defined in the electron density owing to mobility or disorder. The structure of this complex is essentially the same as that previously reported for the 18-residue complex (Gu, Rehman *et al.*, 2012), but the conventional nature of this refinement facilitated by the well ordered crystals allows us to confidently give a full description of the molecular details of binding. The complex is dominated by hydrophobic interactions and is therefore expected to be of reasonably high affinity. The most prominent electrostatic interaction is between the N-terminal helix-capping residue Asp107^{OutS} and the helix dipole of the secretin peptide (Thr693^{OutD}–Tyr705^{OutD}).

The secretin helix (Thr693^{OutD}–Tyr705^{OutD}) is amphipathic, with the hydrophobic residues forming an extended hydrophobic patch along one side of the helix that binds to the hydrophobic concave surface of the pilotin (Fig. 2). The hydrophobic residues of the secretin peptide are, in descending order of contribution to the binding according to *PISA* (Krissinel & Henrick, 2007; Krissinel, 2010), Phe704^{OutD}, Phe694^{OutD}, Val697^{OutD} and Ile701^{OutD}; these residues form the extended hydrophobic patch along one side of the α-helix. Phe704^{OutD} is absolutely conserved, while Phe694^{OutD}, Ile701^{OutD} and Val697^{OutD} are hydrophobic residues in all

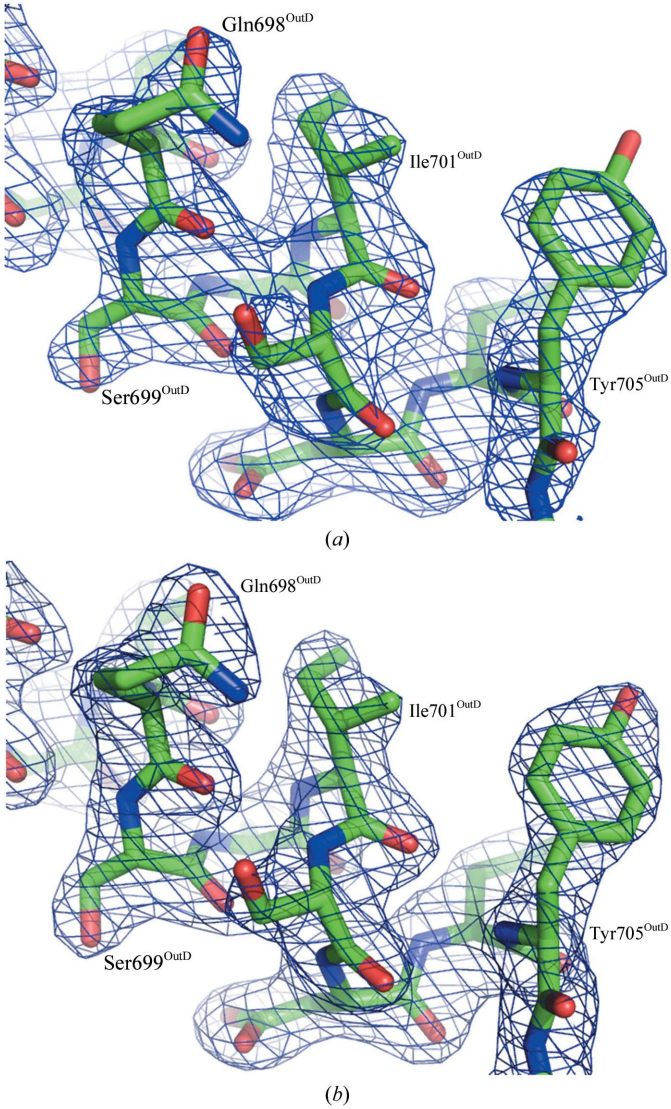

Figure 3
Electron density corresponding to the *D. dadantii* secretin peptide binding to its cognate pilotin. (*a*) σ_A-weighted $2F_{obs} - F_{calc}$ simulated-annealed OMIT map calculated with the secretin peptide omitted and (*b*) σ_A-weighted $2F_{obs} - F_{calc}$ map from the final round of refinement. The electron-density maps, shown as a blue chicken-wire mesh, are contoured at 0.5σ (simulated-annealed OMIT map) and 1.0σ (final map). The secretin peptide numbers have the superscript OutD.

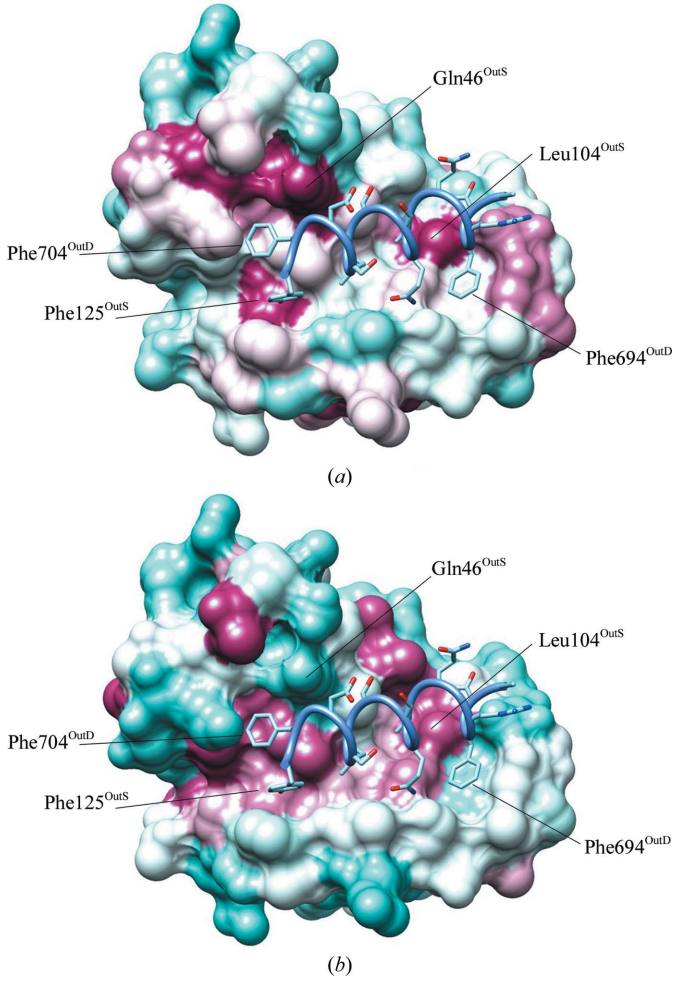

Figure 4
Surface representation of the *D. dadantii* pilotin showing conservation of residues (*a*) and residue hydrophobicity (*b*) of the binding site. The secretin peptide is shown in ribbon representation with side chains. In (*a*) highly conserved residues are shown in burgundy and highly variable residues are shown in cyan. The sequences used are shown in Fig. 1(*b*). In (*b*) hydrophobic residues are coloured burgundy and hydrophilic residues are coloured cyan; these are assigned according to the Kyte and Doolittle hydrophobicity scale (Kyte & Doolittle, 1982). The use of residue hydrophobicity has its limitations, but nonetheless the figure does indicate the hydrophobicity of the binding site.

sequences (Phe or Leu, Ile or Val, and Val, Leu or Ile at positions 694, 701 and 697, respectively).

The secretin peptide binds to the concave surface of the pilotin such that all four helices of the pilotin contribute residues that bind the secretin peptide (Fig. 2). It binds to a region that is well conserved on the surface of the pilotin (Fig. 4*a*). The key pilotin residues involved in the interface are Gln46^{OutS}, Leu47^{OutS}, Ser49^{OutS} and Leu50^{OutS} of α1; Val79^{OutS} of α2; Gly103^{OutS}, Leu104^{OutS} and Asp107^{OutS} of α3; and Gln114^{OutS}, Ser117^{OutS}, Phe118^{OutS}, Thr121^{OutS}, Met122^{OutS}, Pro124^{OutS} and Phe125^{OutS} of α4 (Fig. 2). Of these, Gln46^{OutS}, Leu104^{OutS} and Phe125^{OutS} are conserved (Fig. 4*a*), while the others are semi-conserved. For example, residue 49^{OutS} is either Ser or Ala (a small residue), residue 107^{OutS} is either Asp or Glu (a carboxylic acid side chain) and residue 118^{OutS} is either Phe or Leu (a hydrophobic residue) [the hydrophobicity of the binding site on a residue basis (Kyte & Doolittle, 1982) is shown in Fig. 4*b*].

Phe704^{OutD} of the secretin binds to a hydrophobic cleft between helices α1 and α2 comprising residues Gln46^{OutS} (CH_2 groups), Ser49^{OutS}, Leu50^{OutS} and Val79^{OutS}. Ile701^{OutD} packs against Leu50^{OutS} and Met122^{OutS}, and Val697^{OutD} packs against Leu100^{OutS}, Leu104^{OutS} and Phe118^{OutS}. The small residues on α1 (Ser49^{OutS}, Ala52^{OutS} and Ala53^{OutS}) allow the secretin helix to pack tightly up against the first helix and allow its hydrophobic side chains to pack into hydrophobic pockets on either side of the first helix. According to *PISA*, Ser49^{OutS}, Leu50^{OutS}, Leu100^{OutS}, Leu104^{OutS}, Phe118^{OutS}, Met122^{OutS} and Pro124^{OutS} all contribute at least 0.3 kcal mol^{-1} to the binding energy (Krissinel & Henrick, 2007; Krissinel, 2010).

Asp107^{OutS} acts as an N-terminal helix-capping residue, making hydrogen bonds to the secretin main-chain amides of residues Thr693^{OutD} and Phe694^{OutD} (Supplementary Table 1[1]). This Asp is conserved at this position, except in *Yersinia mollaretii* pilotin where it is a Glu; the glutamate here is assumed to effect a similar helix-capping function, making hydrogen bonds and interacting favourably with the positive end of the helix dipole (Fig. 2). Overall, there are only six hydrogen bonds between the secretin peptide and the pilotin in the complex involving side chains (Supplementary Table 1). The interface area calculated using the 13 ordered residues in *PISA* is 648 Å^2, with a complexation significance score of 1.00. The interface involves 71 and 24 atoms from the pilotin and the secretin peptide, respectively.

There is another conserved patch on the surface of these pilotins (Supplementary Fig. 1). In the crystal lattice the pilotin molecules form a dimer and the conserved patch forms the interface between the pilotin subunits. The significance of the crystallographic dimer is unclear, as the pilotin behaves as a monomer in solution, but the conservation of the dimer interface suggests that the interface is biologically important. This interface comprises mostly charged and polar residues and water molecules, so the interaction may not be strong in solution, but in a more hydrophobic environment, for instance close to a membrane, this interaction may have a greater significance.

Despite the widespread change in the HSQC spectrum (Gu, Rehman *et al.*, 2012), the pilotin undergoes only minor conformational change in response to binding the peptide. This may be because the residues involved in binding are spread throughout the pilotin sequence; several of them are hydrophobic and are involved both in stabilizing the pilotin structure and in binding the secretin peptide, and changes in their electronic properties have widespread effects on the HSQC spectrum. In contrast, the secretin peptide undergoes a profound change in conformation from nonstructured in solution to helical when bound to the pilotin (Gu, Rehman *et al.*, 2012).

The 15-residue peptide does not aggregate as readily as the previously used 18-residue peptide, allowing the thermodynamics of binding to be assessed. The results of isothermal titration calorimetry using the 15-residue peptide agree with the 1:1 stoichiometry of binding seen in the X-ray structure (Figs. 2 and 5). The affinity (K_d) for this 15-residue peptide,

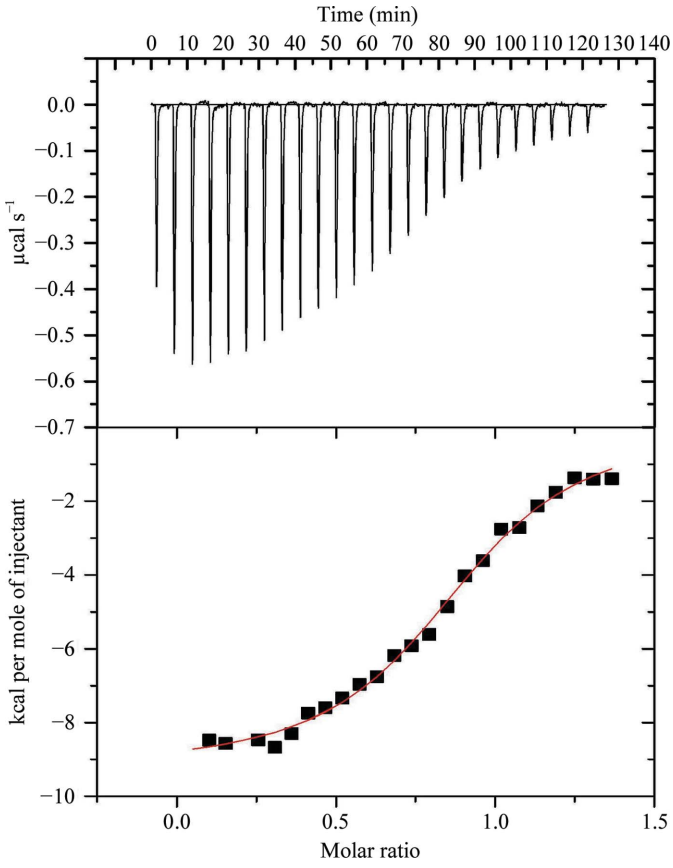

Figure 5
Isothermal titration calorimetry (ITC) analysis of the binding of the secretin peptide to the pilotin. The thermodynamic results from titrating the 15-residue peptide (13 secretin residues plus additional solubilizing residues at the N- and C-termini) into a solution of the pilotin show a 1:1 complex with micromolar affinity. Note that the affinity measured using fluorescence spectroscopy and an 18-residue secretion peptide was higher, but this peptide tended to aggregate and was not suitable for ITC.

[1] Supplementary material has been deposited in the IUCr electronic archive (Reference: YT5051). Services for accessing this material are described at the back of the journal.

with solubilizing terminal residues, is 1.2 ± 0.1 μ*M*. Interestingly, the binding is apparently driven by enthalpy (−9.2 ± 1.4 kcal mol^{-1}) rather than entropy (−3.42 cal mol^{-1} K^{-1}). The loss of conformational entropy of the peptide on binding apparently balances the expected entropy gain from displacing water molecules from the hydrophobic binding surfaces.

In this paper, we have shown precisely how the PulS–OutS family of pilotins bind to their cognate secretin S-domains *via* conserved and semi-conserved hydrophobic interactions. A hydrophobic stripe on the surface of the S-domain α-helix interacts with hydrophobic patches on either side of the first α-helix of the pilotin. The sequence of the PulS–OutS pilotins is constrained where interaction with the S-domain helix occurs, notably where the S-domain helix binds tightly up against small residues on the surface of the first helix and the hydrophobic binding patches on either side of this helix. A conserved carboxylate interacts favourably with the helix dipole and hydrogen bonds to the N-terminal helix amides. This interaction, combined with the hydrophobic interactions, drives the previously unstructured S-domain to form an α-helix when bound to the surface of the pilotin.

We acknowledge funding from BBSRC (BB/I013334/1), HEFCE and Queen Mary University of London. VS was supported by a grant from the French ANR-2010-BLANC-1531 SecPath programme. We acknowledge the use of the PROXIMA1 beamline at SOLEIL for X-ray data collection. We thank the Co-editor for excellent advice resulting in an improved manuscript.

References

Adams, P. D. *et al.* (2010). *Acta Cryst.* D**66**, 213–221.
Bayan, N., Guilvout, I. & Pugsley, A. P. (2006). *Mol. Microbiol.* **60**, 1–4.
Berry, J.-L., Phelan, M. M., Collins, R. F., Adomavicius, T., Tønjum, T., Frye, S. A., Bird, L., Owens, R., Ford, R. C., Lian, L.-Y. & Derrick, J. P. (2012). *PLoS Pathog.* **8**, e1002923.
Chami, M., Guilvout, I., Gregorini, M., Rémigy, H. W., Müller, S. A., Valerio, M., Engel, A., Pugsley, A. P. & Bayan, N. (2005). *J. Biol. Chem.* **280**, 37732–37741.
Collin, S., Guilvout, I., Nickerson, N. N. & Pugsley, A. P. (2011). *Mol. Microbiol.* **80**, 655–665.
DeLano, W. L. & Lam, J. W. (2005). *Abstr. Pap. Am. Chem. Soc.* **230**, U1371–U1372.
Douzi, B., Filloux, A. & Voulhoux, R. (2012). *Philos. Trans. R. Soc. B Biol. Sci.* **367**, 1059–1072.
Dunstan, R. A., Heinz, E., Wijeyewickrema, L. C. Pike, R. N., Purcell, A. W., Evans, T. J., Praszkier, J., Robins-Browne, R. M., Strugnell, R. A., Korotkov, K. V. & Lithgow, T. (2013). *PLoS Pathog.* **9**, e1003117.
Emsley, P., Lohkamp, B., Scott, W. G. & Cowtan, K. (2010). *Acta Cryst.* D**66**, 486–501.
Evans, P. (2006). *Acta Cryst.* D**62**, 72–82.
Filloux, A. (2004). *Biochim. Biophys. Acta*, **1694**, 163–179.
Gu, S., Kelly, G., Wang, X., Frenkiel, T., Shevchik, V. E. & Pickersgill, R. W. (2012). *J. Biol. Chem.* **287**, 9072–9080.
Gu, S., Rehman, S., Wang, X., Shevchik, V. E. & Pickersgill, R. W. (2012). *PLoS Pathog.* **8**, e1002531.
Guilvout, I., Chami, M., Engel, A., Pugsley, A. P. & Bayan, N. (2006). *EMBO J.* **25**, 5241–5249.
Hardie, K. R., Lory, S. & Pugsley, A. P. (1996). *EMBO J.* **15**, 978–988.
Kabsch, W. (2010). *Acta Cryst.* D**66**, 125–132.
Korotkov, K. V., Gonen, T. & Hol, W. G. J. (2011). *Trends Biochem. Sci.* **36**, 433–443.
Korotkov, K. V., Johnson, T. L., Jobling, M. G., Pruneda, J., Pardon, E., Héroux, A., Turley, S., Steyaert, J., Holmes, R. K., Sandkvist, M. & Hol, W. G. J. (2011). *PLoS Pathog.* **7**, e1002228.
Korotkov, K. V., Sandkvist, M. & Hol, W. G. J. (2012). *Nature Rev. Microbiol.* **10**, 336–351.
Krissinel, E. (2010). *J. Comput. Chem.* **31**, 133–143.
Krissinel, E. & Henrick, K. (2007). *J. Mol. Biol.* **372**, 774–797.
Kyte, J. & Doolittle, R. F. (1982). *J. Mol. Biol.* **157**, 105–132.
Laskowski, R. A., MacArthur, M. W., Moss, D. S. & Thornton, J. M. (1993). *J. Appl. Cryst.* **26**, 283–291.
Login, F. H., Fries, M., Wang, X., Pickersgill, R. W. & Shevchik, V. E. (2010). *Mol. Microbiol.* **76**, 944–955.
Murshudov, G. N., Skubák, P., Lebedev, A. A., Pannu, N. S., Steiner, R. A., Nicholls, R. A., Winn, M. D., Long, F. & Vagin, A. A. (2011). *Acta Cryst.* D**67**, 355–367.
Nickerson, N. N., Tosi, T., Dessen, A., Baron, B., Raynal, B., England, P. & Pugsley, A. P. (2011). *J. Biol. Chem.* **286**, 38833–38843.
Okuda, S. & Tokuda, H. (2011). *Annu. Rev. Microbiol.* **65**, 239–259.
Peabody, C. R., Chung, Y. J., Yen, M.-R., Vidal-Ingigliardi, D., Pugsley, A. P. & Saier, M. H. Jr (2003). *Microbiology*, **149**, 3051–3072.
Reichow, S. L., Korotkov, K. V., Hol, W. G. J. & Gonen, T. (2010). *Nature Struct. Mol. Biol.* **17**, 1226–1232.
Sandkvist, M. (2001). *Mol. Microbiol.* **40**, 271–283.
Shevchik, V. E. & Condemine, G. (1998). *Microbiology*, **144**, 3219–3228.
Strozen, T. G., Li, G. & Howard, S. P. (2012). *Infect. Immun.* **80**, 2608–2622.
Thanassi, D. G. & Hultgren, S. J. (2000). *Curr. Opin. Cell Biol.* **12**, 420–430.
Tokuda, H. & Matsuyama, S. (2004). *Biochim. Biophys. Acta*, **1694**, IN1–IN9.
Tosi, T., Nickerson, N. N., Mollica, L., Jensen, M. R., Blackledge, M., Baron, B., England, P., Pugsley, A. P. & Dessen, A. (2011). *Mol. Microbiol.* **82**, 1422–1432.
Wang, X., Pineau, C., Gu, S., Guschinskaya, N., Pickersgill, R. W. & Shevchik, V. E. (2012). *J. Biol. Chem.* **287**, 19082–19093.
Weiss, M. S. (2001). *J. Appl. Cryst.* **34**, 130–135.